arXiv:astro-ph/0506710v1 28 Jun 2005

To appear Spitzer Special Issue, ApJS

Is the Cepheus E Outflow driven by a Class 0 Protostar?

Alberto Noriega-Crespo[1], Amaya Moro-Martin[2], Sean Carey[1], Patrick W. Morris[1], Deborah L. Padgett[1], William B. Latter[1], James Muzerolle[2]

ABSTRACT

New early release observations of the Cepheus E outflow and its embedded source, obtained with the Spitzer Space Telescope, are presented. We show the driving source is detected in all 4 IRAC bands, which suggests that traditional Class 0 classification, although essentially correct, needs to accommodate the new high sensitivity infrared arrays and their ability to detected deeply embedded sources. The IRAC, MIPS 24 and 70μm new photometric points are consistent with a spectral energy distribution dominated by a cold, dense envelope surrounding the protostar. The Cep E outflow, unlike its more famous cousin the HH 46/47 outflow, displays a very similar morphology in the near and mid-infrared wavelengths, and is detected at 24μm. The interface between the dense molecular gas (where Cep E lies) and less dense interstellar medium, is well traced by the emission at 8 and 24 μm, and is one of the most exotic features of the new IRAC and MIPS images. IRS observations of the North lobe of the flow confirm that most of the emission is due to the excitation of pure H_2 rotational transitions arising from a relatively cold ($T_{ex} \sim 700$ K) and dense ($N_H \sim 9.6 \times 10^{20}$ cm^{-2}) molecular gas.

Subject headings: ISM: Herbig-Haro objects — ISM: individual (Cep E) — ISM: jets and outflows — ISM: molecules — infrared: stars — stars: formation

1. Introduction

Class 0 objects were defined a decade ago (André, Ward-Thompson & Barsony 1993) as those protostellar objects undergoing a gravitational collapse. They are characterized

[1]SPITZER Science Center, California Institute of Technology, CA 91125 USA

[2]Steward Observatory, University of Arizona, 933 N Cherry Ave, AZ 85721 USA

by strong submillimeter continuum emission and relatively weak or 'non existent' infrared emission shortward of $\sim 10\mu$m (André, Ward-Thompson, & Barsony 2000). Observationally, all the known Class 0 objects show traces of active mass loss in the form of outflows (André, Ward-Thompson & Barsony 2000), and therefore, theoretical schemes to describe their evolution invoke a delicate balance between mass accretion (to form the star) and mass loss, to drive the outflow and remove angular momentum to sustain the star formation process (Smith 1998; Myers et al. 1998; Smith 2000; Froebrich et al. 2003).

The Cepheus E (Cep E) outflow and its driving source are considered a very good example for studying this interface between the protostar and its mass loss, given the youth of its outflow, with a dynamical age of ~ 5000 yr, and the strength of its millimeter continuum emission, 1 Jy at 1.3mm (Chini et al. 2001; Lefloch, Eislöeffel & Lazareff 1996). At a distance of 730 pc, Cep E-mm is one of the brightest Class 0 protostars known, and likely to become an intermediate ($\sim 3\,M_{\odot}$) mass star (Moro-Martin et al. 2001; Froebrich et al. 2003).

Cep E was first identified as an outflow based on millimeter CO observations (Sargent 1977; Fukui 1989), followed by near infrared and higher spatial resolution CO studies (Hodapp 1994; Eislöffel et al. 1996; Ladd & Hodapp 1997; Ladd & Howe 1997b; Noriega-Crespo, Garnavich & Molinari 1998). The outflow itself is quite compact, $\sim 1.5'$, and driven by the IRAS 23011+6126 source, also known as Cep E-mm. The outflow is deeply embedded and nearly invisible at visible wavelengths, with the exception of its South lobe which is breaking through the molecular cloud (Noriega-Crespo 1997; Devine, Reipurth & Bally 1997; Ayala et al. 2000; Noriega-Crespo & Garnavich 2001) and is named Herbig-Haro (HH) object 377. The properties of the outflow have been thoroughly analyzed in two recent studies (Moro-Martin et al. 2001; Smith, Froebrich & Eislöffel 2003). A comparative study of Cep E-mm source, in the context of other well known Class 0/I sources, was recently carried by Froebrich et al. (2003). We will rely on these works for the interpretation of the Spitzer observations.

In this *Letter* we present new data on the Cep E source and outflow obtained with the Spitzer Space Telescope using its three instruments aboard. A brief description of the observations is presented in § 2, in § 3 is the analysis of the data, and in § 4 we summarize our results.

2. Observations

The Spitzer Cep E data were obtained during the in-orbit checkout and Science Verification period. Cep E was observed using MIPS (Rieke et al. 2004) on 2003 Nov 29, IRAC

(Fazio et al. 2004) on Nov 26 and IRS (Houck et al. 2004) on Nov 29. The MIPS observations were performed in photometry mode at 24μm and fine scale 70μm, with 3 and 10 sec frame times respectively, and a total integration time of ∼48 and 167 sec, accordingly. The IRAC observations used high dynamic range 12 sec frames with an on-source time of 108 sec. The IRS observations are of the North section of embedded outflow ($\alpha = 23^h03^m13.6^s$, δ=+61°42′43.5″ J2000). The spectroscopic observations were tuned to obtain a high signal-to-noise ratio (> 50) spectrum over the 5.5 to 37μm wavelength range, based on our previous knowledge of the Cep E mid-IR emission (Moro-Martin et al. 2001). Ramp durations of the different IRS modules were adjusted to achieve this. The data from the 3 instruments were processed with the Spitzer Science Center Pipeline S9.5[1] which provides the basic calibrated data, the starting point for further analysis. The IRS spectra was analyzed using ISAP [2].

3. Results and Discussion

3.1. The IRAC-MIPS Morphology and Photometry

Figure 1 shows an image of Cep E in the near-IR vibrational line H_2 v = 1–0 S(1) at 2.12μm (Noriega-Crespo, Garnavich & Molinari 1998) over a 2′ FOV; the position of the IRAS 23011+6126 (Cep E-mm) is marked with a cross. A composite image using the four IRAC channels is shown in Figure 2. At first sight the morphology of outflow in the H_2 near infrared emission is remarkably similar to that at 3.6, 4.5, 5.7 and 8μm. Some noticeable differences are (i) the embedded driving source is bright and undoubtly detected, (ii) there are some fan structures at the base of both outflow lobes, (iii) the H_2 emission (green color) is the dominant component (see below), and (iv) the edge of the cloud , where HH 377 is visible, is traced by the 8μm emission (red color) and is probably related to the 7.7μm PAH feature.

A similar, and a bit more ambitious because of large wavelength range coverage, is the comparison shown in Fig. 3, where the H_2 2.12μm, IRAC 4.5μm and MIPS 24μm emission are shown together. The comparison is relevant because it shows the presence of the outflow at 24μm, despite the very bright source, and a larger extension of the warm dust at the edge of the cloud (red color). We performed photometric measurements of the Cep E-mm source using IDP3[3], including PSF-fitting with apertures ∼ 6″ for the IRAC channels, and

[1]http://ssc.spitzer.caltech.edu/postbcd/

[2]http://www.ipac.caltech.edu/iso/isap/isap.html

[3]http://mips.as.arizona.edu/MIPS/IDP3/

tuning the sky background measurements to the extended emission from the outflow, which happens to be insignificant in relationship with the flux of the source (see below). The MIPS measurements at 24 and 70μm include the outflow emission, but this contamination is estimated to be less than 1%. The integrated fluxes for the source are in Table 1, the formal uncertainties on the measurements are $\sim$ 10% for IRAC and MIPS 24μm. For the 70μm fine scale measurement the uncertainty is likely to be higher, 20%, mostly because the source is near the edge of the good part of array and we are underestimating the flux even after the aperture correction.

The spectral energy distribution (SED) using previous and Spitzer measurements is shown in Fig. 4, and is compared also with a very simple SED model. The model has been described in detail elsewhere (Noriega-Crespo, Garnavich & Molinari 1998). It is based on an envelope made of spherically symmetry dust shells where the temperature and density are assumed to follow a power law and exponents of these mathematical relations are adjusted to fit the observations. The model in Fig. 4 has identical parameters as those in Moro-Martin et al. (2001), which uses silicates as the main component of the dust grains, and therefore, produces big absorption bands at 10 and 20μm. One of the reasons why we adopted this model was the fact that ISOCAM observations did not detect the source at 9.6μm (Noriega-Crespo, Garnavich & Molinari 1998). The model SEDs in Fig. 4 are only meant to illustrate what is expected from an dust envelope model and to bring into context the new IRAC and MIPS measurements. There is the concern that the IRAC measurements could be contaminated by shock emission from the outflow. In Cep E-mm source this certainly could be the case if a large aperture ($> 6''$) is used (see e.g. Engelke at al. 2004, Fig. 10). Figure 5 shows the CVF ISOCAM spectrum of Cep E-mm, the spectrum was extracted from a single $6'' \times 6''$ pixel, and shows strong silicate, H_2O and CO_2 absorption features, characteristic of a deeply embedded source, but not traces of H_2 emission from the outflow itself (Moro-Martin et al. 2001). We believe, therefore, that any light contribution from the outflow in the Cep E-mm source IRAC measurements is negligible in this case. The dust envelope SED model predicts a mass of $\sim$13 $M_\odot$ and a bolometric luminosity of $\sim$30 $L_\odot$. SED models based on a graybody approximation (Froebrich et al. 2003) predict a factor two higher luminosity ($\sim$ 78 $L_\odot$) and temperature ($\sim$ 35 K), although the envelope mass differs only by 25% ($\sim$8 $M_\odot$) with respect to our model.

We have pointed out before (Cernicharo et al. 2000) that despite the many magnitudes of absorption produced by the dense envelopes surrounding Class 0 protostars and the presence of deep absorption features from silicate dust and ices, that is possible to detect low mass Class 0 protostars at shorter wavelengths than 10μm, given the high sensitivity of infrared arrays in space. This is relevant because of large surveys which are being performed by the Spitzer Legacy projects, aiming to provide a complete census of the low end of the mass

spectrum in nearby molecular clouds (Evans et al. 2003), and should be taken in to account when a protostar class is assigned.

3.2. H_2 Emission from Cep E North

The IRS observations of the outflow were taken at the brightest region of the embedded redshifted lobe, as illustrated in Fig. 1. The spectrum of Cep E North is dominated at short wavelengths (<13μm) by the pure H_2 rotational lines (Fig. 6) as expected from previous studies (Moro-Martin et al. 2001; Smith, Froebrich & Eislöffel 2003; Noriega-Crespo 2002). The detection of the H_2 0-0 S(0) 28.22μm and 0-0 S(1) 17.04μm lines is among the first ones in a low mass outflow, and demonstrates the superb sensitivity of the IRS spectrometer. Besides the H_2 rotational lines, two atomic low excitation lines, [SI] at 25.25μm and [SiII] at 34.8μm, are detected. The spectrum shows the 11.3μm PAH band, and there are indications that silicate absorption at 10μm and CO_2 ice at 15.2μm are also present.

The spectrum was dereddened using an E(B-V)= 1, and the measured H_2 integrated fluxes were used to estimate the mean excitation temperature (assuming LTE) and the column density of the emitting molecular gas. We found $T_{ex} = 686 \pm 30$ K and $N_H \sim 9.6 \times 10^{20}$ cm^{-2}, this column density corresponds to a number density of $\sim 6.4 \times 10^4$ cm^{-3}, assuming an an envelope size of $\sim$ 1000 AU (Moro-Martin et al. 2001).

Studies of the mid and far-infrared emission from the Cep E outflow (Moro-Martin et al. 2001; Smith Froebrich & Eislóffel 2003) essentially agree with the scenario in which low velocity C-type shocks are the main excitation mechanism. Based on the relative strength of the H_2 lines and our estimate of the gas density, we derive a mean shock velocity of $\sim$ 20 km s^{-1} for the North outflow lobe (Kaufman & Neufeld 1996). However, the complex morphology of Cep E flow, which is made of multiple knots (Ladd & Hodapp 1997), may require as many as 20 C-type bowshocks to explain the integrated emission of their lobes (Smith, Froebrich & Eislöffel 2003).

4. Summary

We presented new observations of the Cep E outflow and its protostellar source, using the 3 instruments aboard the Spitzer Space Telescope. We found that:

(1) The morphology of the outflow is remarkably similar to that of the near infrared observations. Considering that Cep E provides the second example of a low mass outflow observed with Spitzer (the other one being HH 46/47), we can speculate that outflows

from Class 0 sources do not develop a "loop" or a "bubble" structure (Noriega-Crespo et al. 2004), perhaps because they are in the initial phase of breaking through their dense placental envelope and futher ejection events are required to develop a cavity.

(2) The Cep E-mm source or IRAS 23011+6126 was detected in all four IRAC channels. Considering that the Cep E system lies at a distance of 730 pc, this suggests that our traditional definition of a Class 0 source needs to accommodate the higher sensitivity measurements, at wavelengths shorter than 10μm, achievable with the new generation of infrared arrays in space.

(3) The IRAC and MIPS integrated fluxes of Cep E-mm source are consistent with the Class 0 envelope models, although in detail our simple SEDs models do not fit the IRAC points. A comparison of the 5.7 and 8μm IRAC measurements with the Cep E-mm ISOCAM CVF spectrum shows a very good agreement.

(4) The IRS spectroscopic observations of the redshifted North lobe show a rich spectrum of H_2 pure rotational lines, including strong S(1) 17.04 and S(0) 28.22μm lines. Assuming LTE we used these lines to estimate an excitation temperature of $\sim$ 700K and a column density of $N_H \sim 9.6 \times 10^{20}$ cm^{-2} for a collisionally excited molecular gas. A comparison with C-type shock models, using the H_2 line ratios and a gas density of 10^5 cm^{-3}, gives a mean shock velocity of 20km s^{-1}, consistent with previous estimates.

This work is based on observations made with the Spitzer Space Telescope, which is operated by the Jet Propulsion Laboratory, California Institute of Technology under NASA contract 1407. ANC's research was partially supported by NASA-APD Grant NRA0001-ADP-096. AAH is supported by the Spanish Program Nacional de Astronomía y Astrofísica under grant AYA2002-01055.

REFERENCES

André, Ward-Thompson, D., & Barsony, M. 1993, ApJ, 406, 112

André, Ward-Thompson, D., & Barsony, M. 2000 in Protostars and Planets IV. Tucson: University of Arizona Press; eds Mannings, V., Boss, A.P., Russell, S. S., p. 59

Ayala, S., Noriega-Crespo, A., Garnavich, P., Curiel, S., Raga, A.C., & Böhm K.H. 2000, AJ, 120, 909

Cernicharo, J., Noriega-Crespo, A., Cesarsky, D., Lefloch, B., Gonzalez-Alfonso, E., Najarro, P., Dartois, E., & Cabrit, S. 2000, Science, 288, 649

Chini, R., Ward-Thompson, D., Kirk, J. M., Nielbock, M., Reipurth, B., & Sievers, A. 2001, A&A, 369, 155

Devine, D., Reipurth B., & Bally J. 1997 in "Low Mass Star Formation from Infall to Outflow" Ed. F. Malbet & A. Castets, p91

Eislöffel, J., Smith, M.D., Davis, C.J., & Ray, T.P. 1996, AJ, 112, 2086

Fazio, G., et al. 2004, ApJ submitted

Engelke, C. W., Kramer, K. E., & Price, S. D. 2004, ApJSS, 150, 343

Evans, N. J., Allen, L. E., Blake, G. A., Boogert, A. C. A., Bourke, T., Harvey, P. M., Kessler, J. E., Koerner, D. W., Chang, W. L., Mundy, L. G., Myers, P. C., Padgett, D. L., Pontoppidan, K., Sargent, A. I., Stapelfeldt, K. R., van Dishoeck, E. F., Young, Ch. H., & Young K. E. 2003, PASP, 115, 965

Froebrich, D., Smith, M. D., Hodapp, K.-W., & Eislöffel, J. 2003, MNRAS, 346, 163

Fukui, Y. 1989, in "Low Mass Star Formation and Pre-Main Sequence Objects", ESO 1989, ed. B. Reipurth, p95

Hodapp, K.-W. 1994, ApJSS, 94, 615

Houck, J. et al. 2004, ApJ submitted

Kaufman, M., & Neufeld, D. A. 1996, ApJ, 456, 611

Ladd, E.F., & Hodapp, K. 1997, ApJ, 474, 749

Ladd, E.F., & Howe, J.E. 1997 in "Low Mass Star Formation from Infall to Outflow" Ed. F. Malbet & A. Castets, p145

Lefloch, B., Eislöffel, J.,& Lazareff, B. 1996, A&A, 313, L17

Moro-Martin, A., Noriega-Crespo, A., Molinari, S., Testi, L., Cernicharo, J., & Sargent, A. 2001, ApJ, 555, 146

Myers, P.C., Adams, F. C., Chen, H., & Schaff, E. 1998, ApJ, 492, 703

Noriega-Crespo, A. 1997, in "Herbig-Haro Flows and the Birth of Low Mass Stars" Ed. B. Reipurth & C. Bertout, p103

Noriega-Crespo, A., Garnavich, P. M., & Molinari, S. 1998, AJ, 116, 1388

Noriega-Crespo, A., & Garnavich, P. M. 2001, AJ, 122, 3317

Noriega-Crespo, A. 2002, in Emission Lines from Jets Flows, ed. W.J. Henney, W. Steffen, A. C. Raga, & L. Binette, RMxAC, 13, 71

Noriega-Crespo, A., Morris, P., Marleau, F. R., Carey, S., Boogert, A., van Dishoeck, E.,Evans, N. J., Keene, J., Muzerolle, J., Stapelfeldt, K., Pontoppidan, K., Lowrance, P., Allen, L., & Bourke, T. L. 2004, ApJ submitted

Rieke, G. H., et al. 2004, ApJ submitted

Sargent, A. 1977, ApJ, 218, 736

Smith, M. D. 1998, A&SpS, 261, 169

Smith, M. D. 2000, IrAJ, 27 255

Smith, M. D., Froebrich, D., & Eislöffel, J. 2003, ApJ, 592, 245

This preprint was prepared with the AAS LaTeX macros v5.2.

Table 1. Integrated mid and far-infrared fluxes[a] of the Cep E-mm source for the 4 IRAC channels, MIPS 24 and (fine scale) 70μm bands.

Wavelength[b]	3.5	4.6	5.7	8	24	70
	4.5	29	75	140	3600	30500

[a]in milliJansky

[b]Bandpass reference wavelength in μm

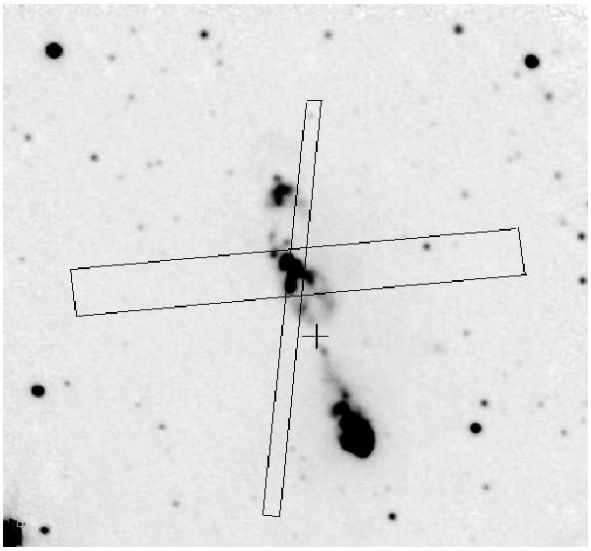

Fig. 1.— Cep E outflow in H_2 at 2.12μm . The image shows the schematic position of the Cep E-mm source (cross) and the Short-Low and Long-low IRS slits. The map shows a $2' \times 2'$ field. N is up and E is to the left.

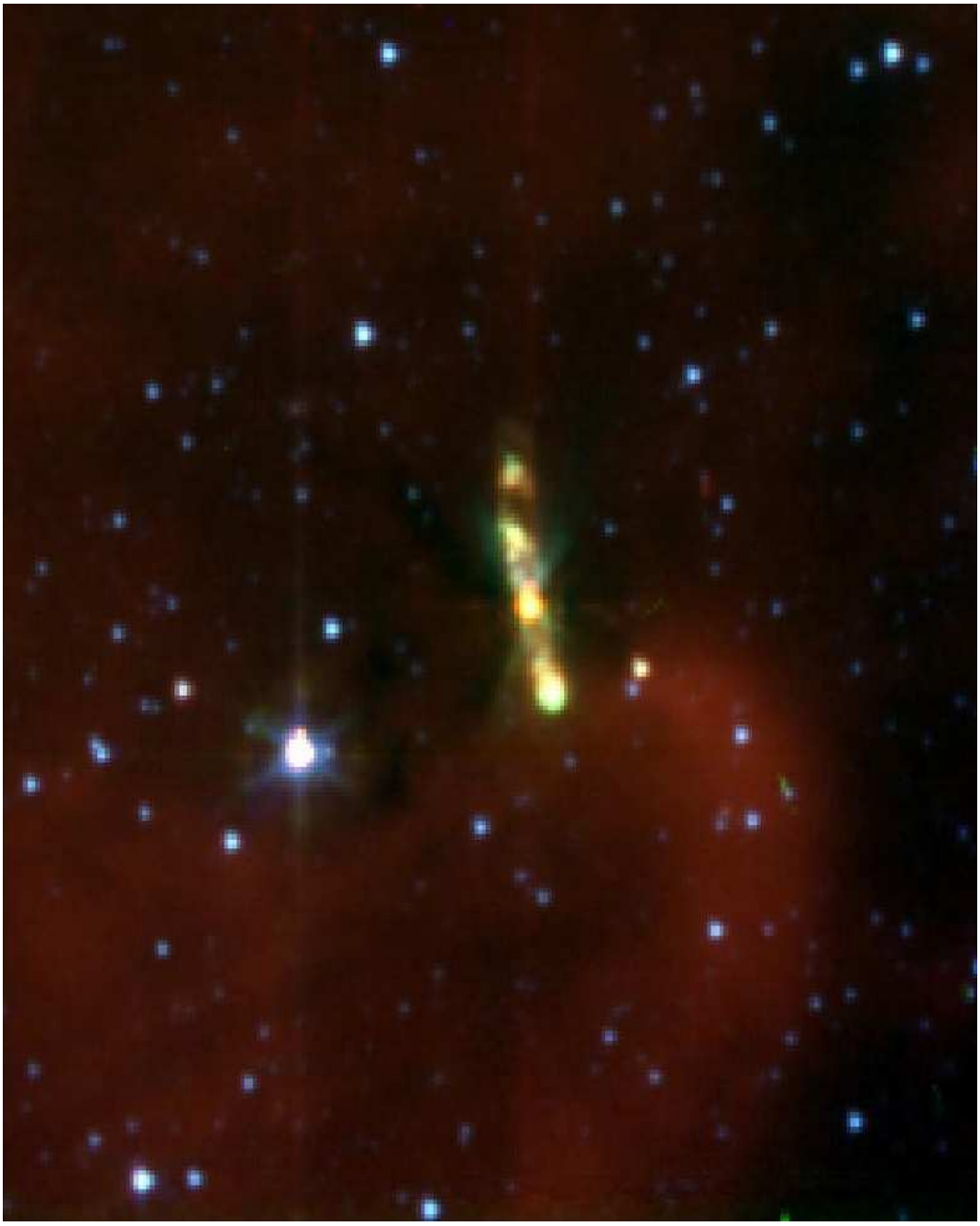

Fig. 2.— [Color Plate] Spitzer image of the Cepheus E embedded outflow obtained using IRAC; the color scheme is the following: 3.6μm (blue), 4.5+5.8μm (green) and 8.0μm (red). The image covers a region of $\sim 5' \times 5'$, and oriented with North up and East to the left.

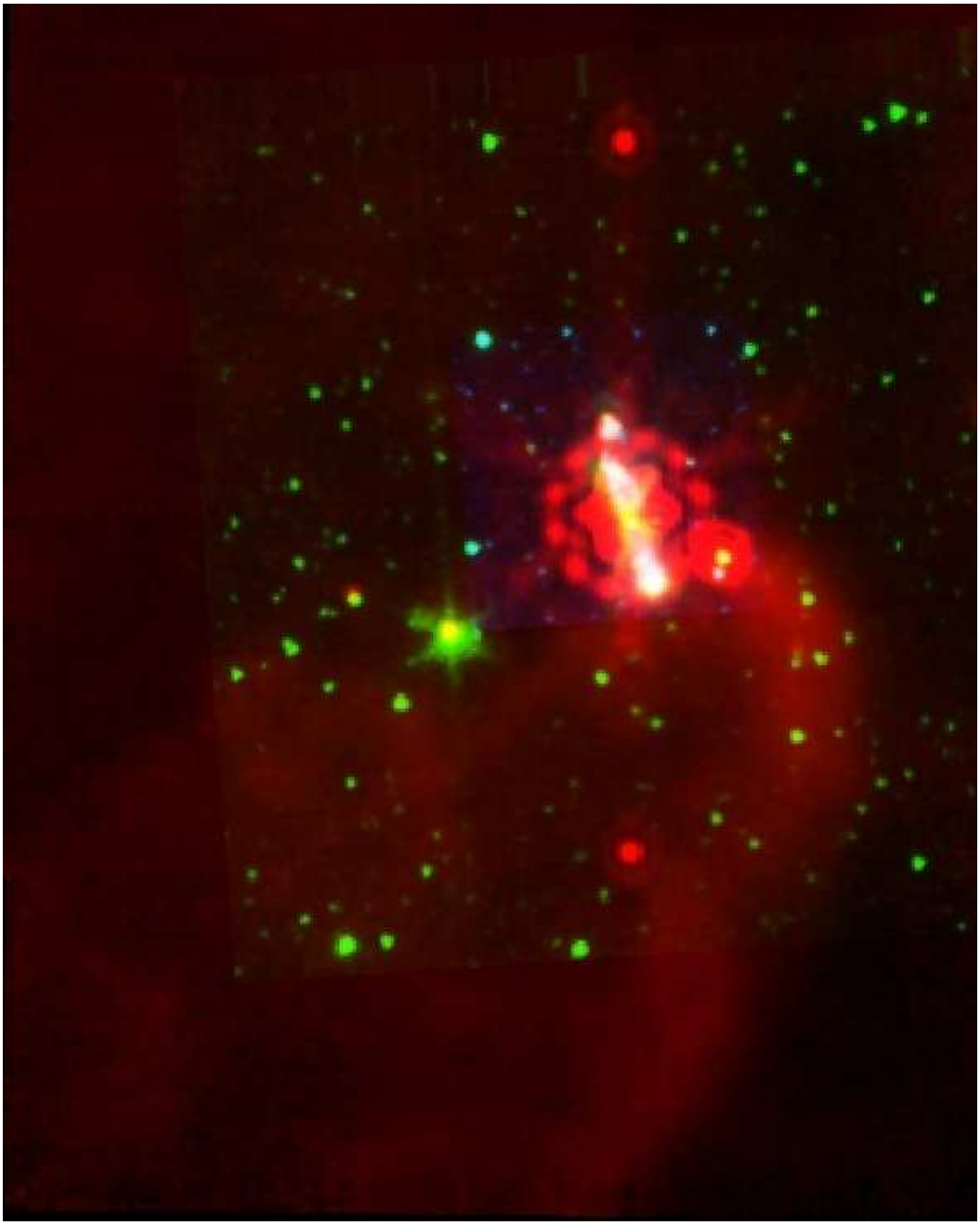

Fig. 3.— [Color Plate] Spitzer image of the Cepheus E embedded outflow obtained using H_2 at 2.12μm (blue), IRAC Channel 2 at 4.5μm (green) and MIPS 24μm (red). The image covers a region of $\sim 5' \times 7'$. North is up and East to the left

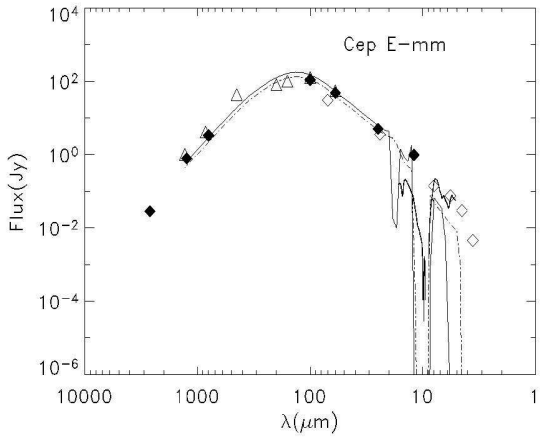

Fig. 4.— Spectral energy distribution of the IRAS 23011+6126 source. Data points are taken from Ladd & Howe 1997 and Noriega-Crespo et al. 1998 (filled diamonds), Froebrich et al. 2003 (open triangles) and IRAC and MIPS measurements in this work (open diamonds). The CVF spectra of Cep E is also included (thick solid line). Two simple models are used for comparison, (1) a model assuming a dust opacity dominated by bare silicates, at a temperature of 18 K and $n = 7.5 \times 10^4$ cm^{-3} (solid line), and (2) a model with $n = 6.4 \times 10^4$ cm^{-3} (broken line), 18 K and dust silicate with a thin ice mantle (Moro-Martin et. al 2001).

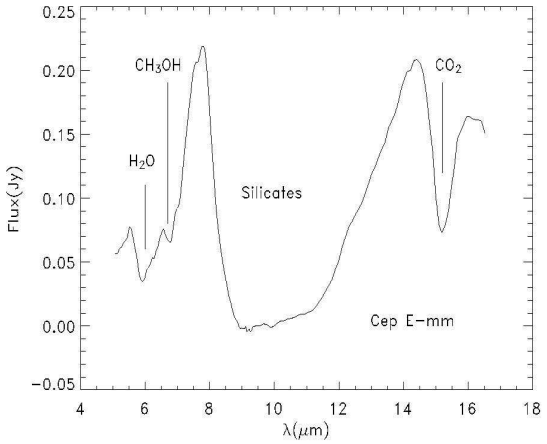

Fig. 5.— Spectrum of Cep E-mm obtained with ISOCAM Circular Variable Filter mode, with some strong silicate and ice absorption features (Moro-Martin et al. 2001).

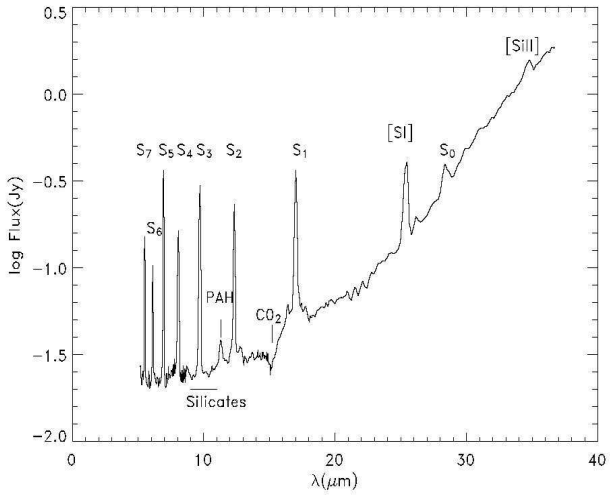

Fig. 6.— IRS spectrum of the North lobe of the Cepheus E embedded outflow.